Evolution of a Functionally Intact but Antigenically Distinct DENV Fusion Loop

Rita M. Meganck[1], Deanna Zhu[2], Stephanie Dong[2], Lisa J. Snoderly-Foster[1], Yago R. Dalben[1], Devina Thiono[3], Laura J. White[3], Aravinda M. DeSilva[3], Ralph S. Baric[2], Longping V. Tse[1]*

[1] Department of Molecular Microbiology and Immunology, Saint Louis University

[2] Department of Epidemiology, University of North Carolina at Chapel Hill

[3] Department of Microbiology, University of North Carolina at Chapel Hill

*Corresponding author: victor.tse@health.slu.edu

ABSTRACT

A hallmark of Dengue virus (DENV) pathogenesis is the potential for antibody-dependent enhancement, which is associated with deadly DENV secondary infection, complicates the identification of correlates of protection, and negatively impacts the safety and efficacy of DENV vaccines. ADE is linked to antibodies targeting the fusion loop (FL) motif of the envelope protein, which is completely conserved in mosquito-borne flaviviruses and required for viral entry and fusion. In the current study, we utilized saturation mutagenesis and directed evolution to engineer a functional variant with a mutated FL (D2-FL) which is not neutralized by FL-targeting monoclonal antibodies. The FL mutations were combined with our previously evolved prM cleavage site to create a mature version of D2-FL (D2-FLM), which evades both prM- and FL-Abs but retains sensitivity to other type-specific and quaternary cross-reactive (CR) Abs. CR serum from heterotypic (DENV4) infected non-human primates (NHP) showed lower neutralization titers against D2-FL and D2-FLM than isogenic wildtype DENV2 while similar neutralization titers were observed in serum from homotypic (DENV2) infected NHP. We propose D2-FL and D2-FLM as valuable tools to delineate CR Ab subtypes in serum as well as an exciting platform for safer live attenuated DENV vaccines suitable for naïve individuals and children.

INTRODUCTION

Dengue virus (DENV) is a member of the *Flavivirus* genus and is a major global public health threat, with four major serotypes of DENV found worldwide. Dengue causes ~400 million infections each year, of which ~20% of cases present clinically, a subset of which may progress to severe Dengue Hemorrhagic Fever/Dengue Shock Syndrome (DHF/DSS).[1,2] DENV is transmitted through *Aedes* mosquito vectors, and globalization and global warming are increasing the endemic range of Dengue worldwide.[3,4] The pathogenesis of Dengue is complex, as first-time infections are rarely severe and lead to serotype-specific immunity. However, re-infection with a different serotype increases the risk of developing DHF/DSS.[5] This is thought to be due to the phenomenon of antibody-dependent enhancement (ADE), in which poorly neutralizing cross-reactive (CR) antibodies (Abs) lead to enhanced viral uptake and infection of unique cell populations in an Fcγ-receptor-mediated manner.[6]

ADE remains a major challenge for DENV vaccine development.[7] The leading DENV vaccine platforms in clinical testing are tetravalent live attenuated virus mixtures of all four serotypes. However, creating formulations that elicit a balanced response has proven challenging.[8] Additionally, lab-grown strains differ from patient-derived DENVs in both maturation status and antigenicity.[9] In particular, Abs targeting the fusion loop (FL) have been reported to neutralize lab and patient strains with differing strengths and have been observed to facilitate Fcγ-receptor uptake *in vitro* and therefore ADE.[10–12] Currently, there is a single FDA-approved DENV vaccine, Dengvaxia. However, it is only approved for use in individuals aged 9-16 with previous DENV infection living in endemic areas and is contraindicated for use in naïve individuals and younger children. In naïve children,

52 vaccination stimulated non-neutralizing CR Abs that increased the risk of severe disease
53 after DENV infection.[13,14] Other DENV vaccines have been tested or are currently
54 undergoing clinical trial, but thus far none have been approved for use in the United
55 States.[15] The vaccine Qdenga has been approved in the European Union, Indonesia, and
56 Brazil, although vaccine efficacy in adults, naïve individuals, and with all serotypes has
57 not yet been shown.

58 The DENV FL is located in Envelope (E) protein domain II (EDII) and is involved
59 in monomer-monomer contacts with EDIII.[16] During the DENV infection cycle, low pH
60 triggers a conformational change in the E protein.[17] The structure of the virion rearranges,
61 and individual monomers form a trimer with all three FLs in the same orientation, ready
62 to initiate membrane fusion.[16,17] The core FL motif (DRGWGNGCGLFGK, AA 98-110) is
63 highly conserved, with 100% amino acid conservation in all DENV serotypes and other
64 mosquito-borne flaviviruses, including Yellow fever virus (YFV), Zika virus (ZIKV), West
65 Nile virus (WNV), Kunjin virus (KUNV), Murray Valley encephalitis virus (MVEV),
66 Japanese encephalitis virus (JEV), Usutu virus (USUV), and Saint Louis encephalitis virus
67 (SLEV; Figure 1A). Although the extreme conservation and critical role in entry have led
68 to it being considered extremely difficult to change the FL, we successfully tested the
69 hypothesis that massively parallel directed-evolution could produce viable DENV FL
70 mutants that were still capable of fusion and entry, while altering the antigenic footprint.
71 The FL mutations, in combination with optimized prM cleavage site mutations, ablate
72 neutralization by the prM- and FL-Abs, retain sensitivity to other protective Abs, and
73 provide a novel vaccine strategy for DENV.
74

RESULTS

To engineer a virus with a novel antigenic footprint at the FL, we targeted the core conserved FL motif. We generated two different saturation mutagenesis libraries, each with 5 randomized amino acids: DRG**X**G**X**G**XXX**FGK (Library 1; AA 101, 103, 105-107) and DRG**XXXXX**GLFGK (Library 2 AA 101-105). Library 1 was designed to mutate known residues targeted by FL mAbs while Library 2 focused on a continuous linear peptide that is the epitope for FL-Abs to maximally alter antigenicity.[18] Saturation mutagenesis plasmid libraries were used to produce viral libraries in either C6/36 (*Aedes albopictus* mosquito) or Vero 81 (African green monkey) cells and passaged three times in their respective cell types. Following directed evolution, viral genomes were extracted and subjected to deep sequencing to identify surviving and enriched variants (Figure 1B). Due to the high level of conservation, it was not surprising that most mutational combinations failed to yield viable progeny. In fact, evolutions carried out on Library 2 only yielded wild-type sequences. For Library 1, wild-type sequences dominated in Vero 81 evolved libraries. However, a novel variant emerged in C6/36 cells with two amino acid changes: DRGWG**S**GC**L**LFGK. The major variant comprised ~95% of the population, while the next most populous variant (DRGWG**S**GC**W**LFGK) comprised only 0.25% (Figure 1C). Bulk Sanger sequencing revealed an additional Env-T171A mutation outside of the FL region. Residues W101, C105, and L107 were preserved in our final sequence, supporting the importance of these residues.[16] When modeled on the pre-fusion DENV2 structure, the N103S and G106L mutations are located at the interface with the neighboring monomer EDIII domain, protected from the aqueous environment. In the post-fusion form, the two residues are located between W101 and F108 and form the

98 bowl concavity above the chlorine ion in the post-fusion trimer (Figure 1D). We used
99 reverse genetics to re-derive the FL N103S/G106L/T171A mutant, which we term D2-FL.
100 As enhancing Abs also target prM,[19] we also created a mature version of D2-FL termed
101 D2-FLM, containing both the evolved FL motif and our previously published evolved prM
102 furin cleavage site, which results in a more mature virion like those found in infected
103 patients (Figure 1E).[9,20]

104 We performed growth curves comparing DENV2, D2-FL, and D2-FLM in both
105 C6/36 and Vero 81 cells. In C6/36 cells, the growth of all three viruses was comparable,
106 reaching high titers of 10^6-10^7 FFU/mL. However, in Vero 81 cells, both FL mutant viruses
107 were highly attenuated, with a 2-2.5 log reduction in titer (Figure 2A). The species-specific
108 phenotype in culture involved a change from insect to mammalian cells, as well as a
109 change in growth temperature. To investigate if the mutant viruses were more unstable
110 at higher temperatures, we performed a thermostability assay, comparing viruses
111 incubated at temperatures ranging from 4-55°C before infection. The three viruses had
112 comparable thermostabilities, indicating that this does not explain the attenuation of the
113 FL mutants (Figure 2B). Because the D2-FLM virus contains mutations that increase prM
114 cleavage frequency, we also assayed the maturation status of the three viruses by
115 western blot. D2-FL had a comparable prM:E ratio to the isogenic wildtype DENV2 (DV2-
116 WT), while, as expected, D2-FLM had a reduced prM:E ratio, indicating a higher degree
117 of maturation (Figure 2C).

118 Next, we characterized the ability of Abs targeting the FL to recognize DV2-WT,
119 D2-FL, and D2-FLM with a panel of monoclonal antibodies (mAbs). Importantly, D2-FL
120 and D2-FLM were resistant to mAbs targeting the FL. Neutralization by 1M7 is reduced

121 by ~2-logs in both variants, 1N5 neutralization is reduced by ~1-log for D2-FL and reduced
122 to background levels for D2-FL, and no neutralization was observed for 1L6 or 4G2 for
123 either variant (Figure 3A).[18] Focusing on the D2-FLM virus containing both evolved motifs,
124 we then characterized the antigenicity of the whole virion with a panel of mAbs. As
125 expected, D2-FLM was unable to be neutralized by the prM Abs 1E16 and 5M22; the Ab
126 2H2 does not neutralize either DV2-WT or D2-FLM (Figure 3B). For Abs targeting
127 epitopes in non-mutated regions, including the ED1 and EDE epitopes that target EDII
128 and EDIII, $FRNT_{50}$ values were generally comparable, although EDE1-C10 shows a
129 moderate but statistically significant reduction between DV2-WT and D2-FLM, indicating
130 that the overall virion structural integrity was intact (Figure 3B).

131 Next, we analyzed neutralization of the D2-FLM virus using serum derived from
132 convalescent humans and experimental infected non-human primates (NHPs). Overall,
133 we tested serum from 6 humans and 9 NHPs at different time points with a total of 27
134 samples. Serum from a homotypic infected NHP (n=3) did not display a difference in
135 neutralization between DV2-WT, D2-FL, and D2-FLM, confirming that prM and FL
136 epitopes are not significant contributors to the homotypic type-specific (TS) neutralizing
137 Ab response in primates (Figure 3C). In heterotypic vaccination and infection, most of the
138 serum (18/24) did not cross-neutralize ($FRNT_{50}$ < 1:40) DV2-WT, confirming the serotypic
139 difference of DENVs (Table 1). However, in two NHPs infected with DENV4, strong
140 neutralization potency ($FRNT_{50}$ between 1: 100 – 1:1,000) was demonstrated against
141 DV2-WT (Figure 3C). Heterologous cross-neutralization was significantly reduced to
142 background levels ($FRNT_{50}$ < 1:40) against the D2-FLM virus at 90 days post-infection
143 (dpi). Of note, one DENV4 animal (3Z6) showed low levels of neutralization against D2-

144 FLM at early time points (20- and 60-days post-infection), which was eventually lost at
145 later time points. Neutralization observed against D2-FL, in general, fell between DV2-
146 WT and D2-FLM. Interestingly, in animal 3Z6, at 20 dpi, neutralization against DENV-FL
147 was comparable to DV2-WT, while D2-FLM was greatly reduced, indicating that
148 antibodies in the sera targeting the immature virion formed a large portion of the CR
149 response. In contrast, animal 0Y0 displayed less difference in neutralization between D2-
150 FL and D2-FLM, suggesting that FL antibodies were more prominent in this animal. These
151 data suggest that after a single infection, much of the CR Ab responses target prM and
152 the FL and tend to wane over time (Figure 3C). The collection of FL, mature, and FL-
153 mature variants provides new opportunity to delineate antibody composition in complex
154 polyclonal serum from DENV natural infection and vaccination.
155

156 **DISCUSSION**

157 Mechanistic understanding of vaccine protection and identification of correlates of
158 protection are immensely important for DENV vaccine development. The dual protective
159 and enhancing properties of DENV Abs create major challenges for dissecting the role of
160 various Ab populations in disease protection. Cross-reactive weakly neutralizing prM- and
161 FL-Abs are often immunodominant after primary DENV infection,[10,21–24] and can lead to
162 overestimation of the levels of heterotypic protection in traditional neutralization assays.
163 Since these same antibodies are also associated with ADE,[19] inaccurate conclusions
164 could have dire consequences if protection *in vitro* translates to the enhancement of
165 disease in human vaccinees. Unfortunately, Ab profiling in polyclonal serum is mainly
166 performed by ELISA, and a neutralization assay that can discriminate Abs does not exist.

167 The D2-FLM variant is not neutralized by FL- and prM-mAbs and appears insensitive to
168 neutralization by these Abs in polyclonal serum. Of note, EDE1-C10 neutralization
169 potency was also reduced in our FL-M variant, further indicating our mutations are
170 affecting the tip of the EDII region which partially overlaps with the EDE1 epitope[25]. In
171 combination with other chimeric DENVs,[26–28] D2-FLM provides a reagent to distinguish
172 between TS, protective CR (e.g. E dimer epitope, EDE),[29,30] and ADE-prone CR (e.g. FL
173 and prM)[24] Ab subclasses in neutralization assays after infection and vaccination.

174 Due to the ADE properties of DENV Abs, studies to understand and eliminate ADE
175 phenotype are under active investigation. For example, mAbs can be engineered to
176 eliminate binding to the Fcγ receptor, abolishing ADE.[31] While this methodology holds
177 potential for Ab therapeutic development and passive immunization strategies, it is not
178 relevant for vaccination. As FL and prM targeting Abs are the major species demonstrated
179 to cause ADE *in vitro* and are thought to be responsible for ADE-driven negative
180 outcomes after primary infection and vaccination,[10–12,32] we propose that genetic ablation
181 of the FL and prM epitopes in vaccine strains will minimize the production of these
182 subclasses of Abs responsible for undesirable vaccine responses. Indeed, efforts have
183 been made to reduce the availability of the FL or reduce the ability of FL Abs to drive
184 ADE. Covalently locked E-dimers and E-dimers with FL mutations have been engineered
185 as subunit vaccines that reduce the availability of the FL, thereby reducing the production
186 of FL Abs.[33–36] DENV subunit vaccines are an area of active study;[37] however,
187 monomer/dimer subunits can also expose additional, interior-facing epitopes not normally
188 exposed to the cell. Furthermore, dimer subunits are not a complete representation of the
189 DENV virion which presents other structurally important interfaces such as the 3-fold and

190 5-fold symmetries. Concerns about balanced immunity to all four serotypes also apply to
191 subunit vaccine platforms. Given the complexity of the immune response to DENV, live
192 virus vaccine platforms have thus far been more successful. However, the fusion loop is
193 strongly mutationally intolerant. Previous reported mutations in the fusion loop of
194 mosquito-borne flaviviruses include a L107F mutation in WNV [38] and JEV associated with
195 attenuation, and mutations at position 106 in ZIKV(G106A) and DENV(G106V) which
196 were tolerated. Interestingly, we also recovered a mutation in position 106 (G106L) Using
197 directed-evolution, we successfully generated our D2-FLM variant that combines viability
198 with the desired Ab responses. Therefore, the D2-FLM variant is a novel candidate for a
199 vaccine strain which presents all the native structures and complex symmetries of DENV
200 necessary for T-cell mediated responses and which can elicit more optimal protective Ab
201 responses.[39–41]

202 Other considerations of high importance when designing a live DENV vaccine
203 include strain selection and serotype balance.[42] In the current study we used DENV2
204 S16803, a prototype for DENV2.[43] However, S16803 was isolated several decades ago,
205 and it may be beneficial to utilize more contemporaneous strains.[8,44] Work is currently
206 ongoing to demonstrate the portability of the evolved FL motif on additional DENV2
207 strains and other serotypes, which is essential for tetravalent vaccine production. D2-FLM
208 was highly attenuated in Vero cells, creating a challenge for vaccine production.
209 Therefore, further adaptation of this strain to grow efficiently in mammalian cells while
210 retaining its antigenic properties is needed. Taken together, the FLM variant holds
211 exciting new possibilities for a new generation of DENV vaccines, as well as a platform
212 to readily measure TS and CR ADE-type responses and thereby assess the true

213 protective potential of any DENV vaccine trials and safeguard approval of DENV vaccines

214 for human use.

ACKNOWLEDGEMENTS

We thank members of the Tse, Baric, and DeSilva laboratories for helpful discussions. This work was supported by NIAID R01AI107731 to A.D. and R.S.B., P01AI106695 to R.S.B., NIAID F30AI160898 to D.R.Z. L.J.W. is supported by NIAID P01 5112869.

AUTHOR CONTRIBUTION

R.M.M. and L.V.T. designed the study. R.M.M. performed high-throughput sequencing preparation and analysis. R.M.M., D.Z., S.D., L.J.S., Y.D., and L.V.T. performed experiments. D.T., L.J.W., A.M.D.S., and R.S.B. provided reagents. L.V.T. and R.S.B. provided oversight of the project and funding. R.M.M. wrote the manuscript. L.V.T. reviewed and revised the final version. All authors approved the final version of the manuscript.

CONFLICT DISCLOSURE

R.M.M., R.S.B., and L.V.T. are inventors on a patent application filed on the subject matter of the manuscript.

231 **MATERIALS AND METHODS**

232 Cells and viruses

233 C6/36 (ATCC CRL-1660) were grown in MEM (Gibco) with 5% FBS (HyClone), 1%
234 penicillin/streptomycin (Gibco), 0.1mM nonessential amino acids (Gibco), 1% HEPES
235 (Gibco), and 2mM GlutaMAX (Gibco), cultured at 32°C with 5% CO_2. Vero 81 cells (ATCC
236 CCL-81) were grown in DMEM/F12 (Gibco) with 10% FBS, 1% penicillin/streptomycin
237 (Gibco), 0.1mM nonessential amino acids (Gibco), and 1% HEPES (Gibco), cultured at
238 37°C with 5% CO_2. DENV viruses were grown in C6/36 or Vero 81 cells maintained in
239 infection media. C6/36 infection media consists of Opti-MEM (Gibco) with 2% FBS
240 (HyClone), 1% penicillin/streptomycin (Gibco), 0.1mM nonessential amino acids (Gibco),
241 1% HEPES (Gibco), and 2mM GlutaMAX (Gibco). Vero 81 infection media consists of
242 DMEM/F12 (Gibco) with 2% FBS, 1% penicillin/streptomycin (Gibco), 0.1mM
243 nonessential amino acids (Gibco), and 1% HEPES (Gibco). DENV2 strain S16803 was
244 used in this study.[43] Sequences used for the alignments include DENV1 WestPac-74
245 (U88535.1), DENV2 S-16803 (GU289914.1), DENV3 3001 (JQ411814.1), DENV4 Sri
246 Lanka-92 (KJ160504.1), YFV 17D (NC_002031.1), SLEV Kern217 (NC_007580.2), JEV
247 (NC_001437.1), USUV Vienna-2001 (NC_006551.1), MVEV (NC_000943.1), WNV-1
248 NY99 (NC_009942.1), and ZIKV MR-766 (NC_012532.1).

249 DENV Reverse Genetics

250 DENV2 S16803 was used in this study. Recombinant viruses were created using a four-
251 plasmid system as previously described,[45] consisting of the DENV genome split into four
252 segments, each cloned into a separate plasmid. The DENV plasmids were digested and
253 ligated to form a single template for *in vitro* transcription. The resulting RNA was

254 electroporated into either C6/36 or Vero cells. Virus-containing supernatant was
255 harvested at 4-5 days post electroporation and passaged. DENV variants were created
256 through site-directed mutagenesis of the DENV plasmids.

257 Library Generation and Directed Evolution

258 DENV fusion loop libraries were generated through saturation mutagenesis of the
259 indicated resides, based on a previously published protocol.[20,46] Degenerate NNK
260 oligonucleotides were used to amplify the region, generating a library of mutated DNA
261 fragments. Q5 DNA Polymerase was used with less than 18 cycles to maintain accuracy.
262 The resulting library was cloned into the DENV reverse genetics system. The ligated
263 plasmids were electroporated into DH10B ElectroMax cells (Invitrogen) and directly
264 plated on 5,245mm^2 dishes (Corning) to avoid bias from suspension culture. Colonies
265 were pooled and purified using a Maxiprep kit (Qiagen), and the plasmid library used for
266 DENV reverse genetics (above). Viral libraries were passaged three times in the
267 corresponding cell type.

268 High-throughput Sequencing and Analysis

269 Viral RNA was isolated with a QIAamp viral RNA kit (Qiagen), and cDNA produced using
270 the Superscript IV Reverse Transcriptase (Invitrogen). Amplicons were prepared for
271 sequencing using the Illumina TruSeq system with two rounds of PCR using Q5 Hot Start
272 DNA polymerase (NEB). For the first round of PCR, primers were specific to the DENV2
273 E sequence surrounding the fusion loop motif with overhangs for the Illumina adapters.
274 After purification, this product was used as the template for the second round of PCR
275 using Illumina P5 and P7 primers containing 8-nucleotide indexes. Purified PCR products
276 were analyzed on a Bioanalyzer (Agilent Technologies) and quantified on a Qubit 4

277 fluorometer (Invitrogen). Amplicon libraries were run on a MiSeq system with 2x150bp
278 reads. Plasmid and P0 libraries were sequenced at a depth of ~4.5 million reads; later
279 passages were sequenced at a depth of ~750,000 reads. Custom perl and R scripts were
280 used to analyze and plot the data as previously published.[20]

281 DENV Growth Kinetics

282 One day before infection, $5x10^5$ cells were seeded in every well of a 6-well plate. Cells
283 with infected with an MOI of 0.05-0.1, estimating $1x10^6$ cells on the day of infection.
284 Infection was carried out for one hour in the incubator, followed by 3x washes with PBS
285 and replenishment with fresh infection medium. 300 uL of viral supernatant was collected
286 at 0, 24, 48, 72, 96, and 120 hours and stored at -80°C. All experiments were performed
287 independently at least three times.

288 DENV Focus-Forming Assay

289 Titers of viral supernatant were determined using a standard DENV focus-forming assay.
290 In brief, cells were seeded at $2x10^4$ cells per well of a 96-well plate one day before
291 infection. The next day, 50 uL of 10-fold serial dilution of viral supernatant were added to
292 each well for 1 hour in the incubator. After, 125uL of overlay (Opti-MEM, 2% FBS, NEAA,
293 P/S, and methylcellulose) was added to each well. Infection was allowed to continue for
294 48 hours in the incubator. Overlay was removed, and each well rinsed 3x with PBS
295 followed by a 30 minute fixation with 10% formalin in PBS. Cells were blocked in
296 permeabilization buffer (eBioscience) with 5% nonfat dried milk. Primary Abs anti-prM
297 2H2 and anti-E 4G2 from nonpurified hybridoma supernatant were used at a 1:500
298 dilution in blocking buffer. Goat anti-mouse HRP secondary (SeraCare KPL) were used
299 at a 1:1000 dilution in blocking buffer. Followed washing, foci were developed using

300 TrueBlue HRP substrate (SeraCare) and counted using an automated Immunospot
301 analyzer (Cellular Technology).

302 Thermal Stability Assay

303 The indicated viruses were thawed and incubated at temperatures ranging from 4°C to
304 55°C for one hour. Following, viral titers were determined by focus-forming assay as
305 described above.

306 Western Blotting

307 Viral supernatants were combined with 4X Laemmli Sample Buffer (Bio-Rad) and boiled
308 at 95°C for 5 minutes. After SDS-PAGE electrophoresis, samples were transferred to
309 PVDF membrane and blocked in 3% nonfat milk in PBS-T. A polyclonal rabbit anti-prM
310 (1:1000; Invitrogen PA5-34966) and polyclonal rabbit anti-Env (Invitrogen PA5-32246) in
311 2% BSA in PBS-T were incubated on the blot for 1 hour at 37C. Goat anti-rabbit HRP
312 (1:10,000 Jackson ImmunoLab) in 3% milk in PBS-T was incubated on the blot for 1 hour
313 at room temperature. Blots were developed by SuperSignal West Pico Plus
314 chemiluminescent substrate (ThermoFisher). Blots were imaged on an iBright FL1500
315 imaging system (Invitrogen). The pixel intensity of individual bands was measured using
316 ImageJ, and the relative maturation was calculated by using the following equation:
317 (prMExp/EnvExp)/(prMWT/EnvWT). All experiments were performed independently a
318 minimum of three times.

319

320 FRNT Assay

321 Focus reduction neuralization titer (FRNT) assays were performed as described
322 previously with C6/36 cells.[20] $1x10^5$ cells were seeded in a 96-well plate the day prior to

323 infection. Abs or sera were serially diluted and mixed with virus (~100 FFU/well) at a 1:1
324 volume and incubated for 1 hour in the incubator. The mixture was added onto the plate
325 with cells and incubated for 1 hour in the incubator, then overlay was added (see Focus-
326 Forming Assay) and plates were incubated for 48 hours. Viral foci were stained and
327 counted as described above (Focus-Forming Assay). A variable slope sigmoidal dose-
328 response curve was fitted to the data, and values were calculated with top or bottom
329 restraints of 100 and 0 using GraphPad Prism version 9.0. All experiments were
330 performed independently at least two times, due to limited amounts of human serum.

331 Statistical Analysis

332 GraphPad Prism version 9.0 was used for statistical analysis. Titer and % infection of D2-
333 FL and D2-FLM were compared to the DV2 using two-way ANOVA. $FRNT_{50}$s were
334 compared using Student's t-test. Significant symbols are as follows: *, $P < 0.05$; **, $P <$
335 0.005; ***, $P < 0.0005$; ****, $P < 0.00005$. The data are graphed as means ± standard
336 deviations.

Figures:

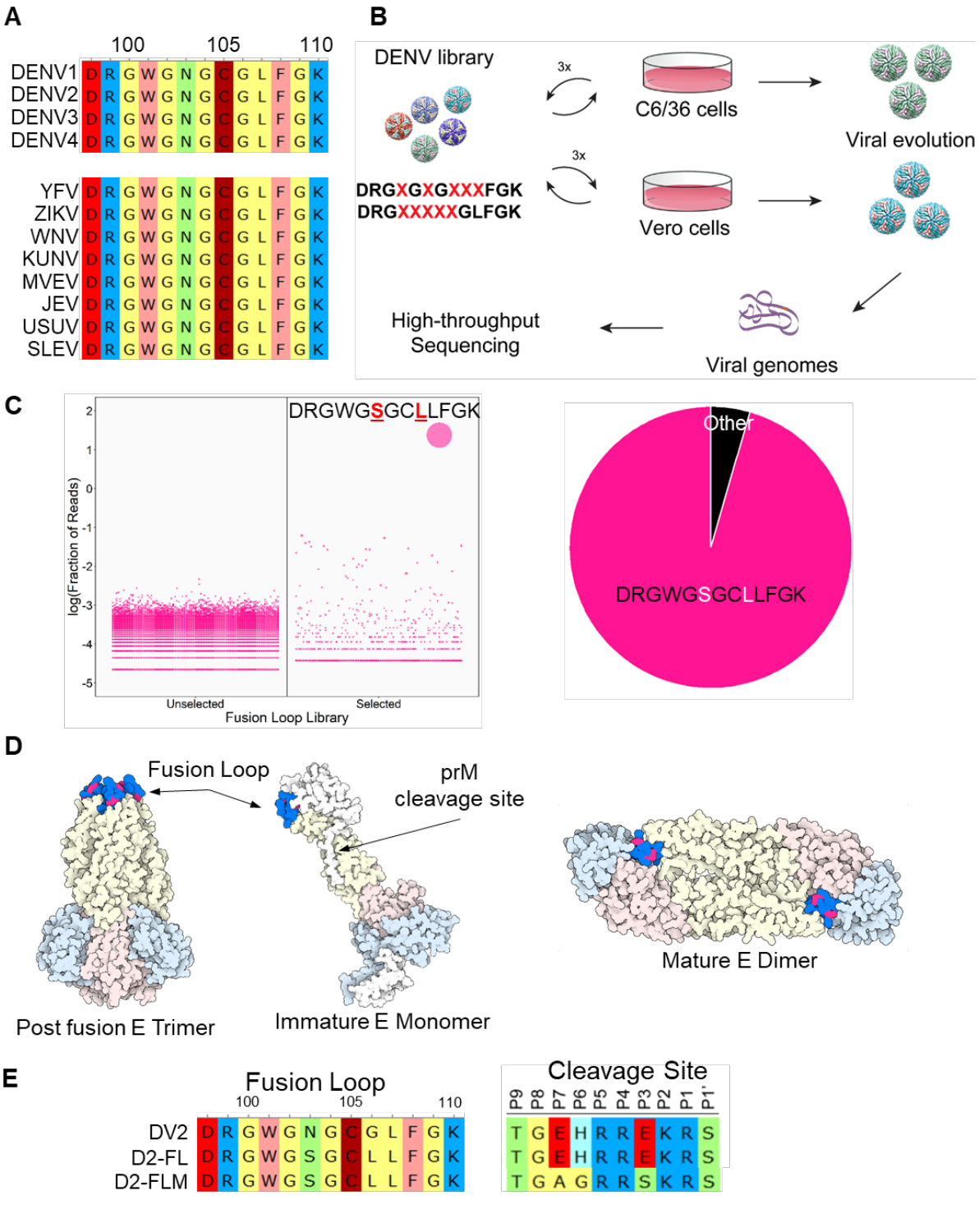
A
100
105
110
DENV1 D R G W G N G C G L F G K
DENV2 D R G W G N G C G L F G K
DENV3 D R G W G N G C G L F G K
DENV4 D R G W G N G C G L F G K
YFV D R G W G N G C G L F G K
ZIKV D R G W G N G C G L F G K
WNV D R G W G N G C G L F G K
KUNV D R G W G N G C G L F G K
MVEV D R G W G N G C G L F G K
JEV D R G W G N G C G L F G K
USUV D R G W G N G C G L F G K
SLEV D R G W G N G C G L F G K
B
DENV library
3x
C6/36 cells
Viral evolution
DRGXGXGXXXFGK
DRGXXXXXGLFGK
3x
Vero cells
High-throughput Sequencing
Viral genomes
C
DRGWGSGCLLFGK
log(Fraction of Reads)
Unselected
Selected
Fusion Loop Library
Other
DRGWGSGCLLFGK
D
Fusion Loop
prM cleavage site
Post fusion E Trimer
Immature E Monomer
Mature E Dimer
E
Fusion Loop
100
105
110
DV2 D R G W G N G C G L F G K
D2-FL D R G W G S G C L L F G K
D2-FLM D R G W G S G C L L F G K
Cleavage Site
P9 P8 P7 P6 P5 P4 P3 P2 P1 P1'
T G E H R R E K R S
T G E H R R E K R S
T G A G R R S K R S

340 **Figure 1**: Generation of DENV2 fusion loop mutants via directed evolution. A) Alignment
341 of Top: Dengue virus fusion loops; Bottom: Mosquito-borne flavivirus fusion loops,
342 including Yellow Fever virus (YFV), Zika virus (ZIKV), West Nile virus (WNV), Kunjin virus
343 (KUNV), Murray Valley Encephalitis virus (MVEV), Japanese Encephalitis virus (JEV),
344 Usutu virus (USUV), and Saint Louis Encephalitis virus (SLEV). Amino acids are colored
345 by functional groups: negatively charged (red), positively charged (blue), nonpolar
346 (yellow), polar (green), aromatic (pink), and sulfide (dark red). B) Schematic of directed
347 evolution procedure. Saturation mutagenesis libraries were used to produce viral libraries,
348 which were passaged three times in either C6/36 or Vero 81 cells. At the end of the
349 selection, viral genomes were isolated and mutations were identified by high-throughput
350 sequencing. C) Left: Bubble plot of the sequences identified from either the unselected
351 or selected (passage 3) C6/36 DENV libraries. Right: Pie chart of the sequences from
352 passage 3 C6/36 DENV libraries. D) Structure of the DENV envelope with the fusion loop
353 mutations highlighted in red. E) Sequences of the fusion loop and furin cleavage site of
354 DENV2, D2-FL, and D2-FLM.

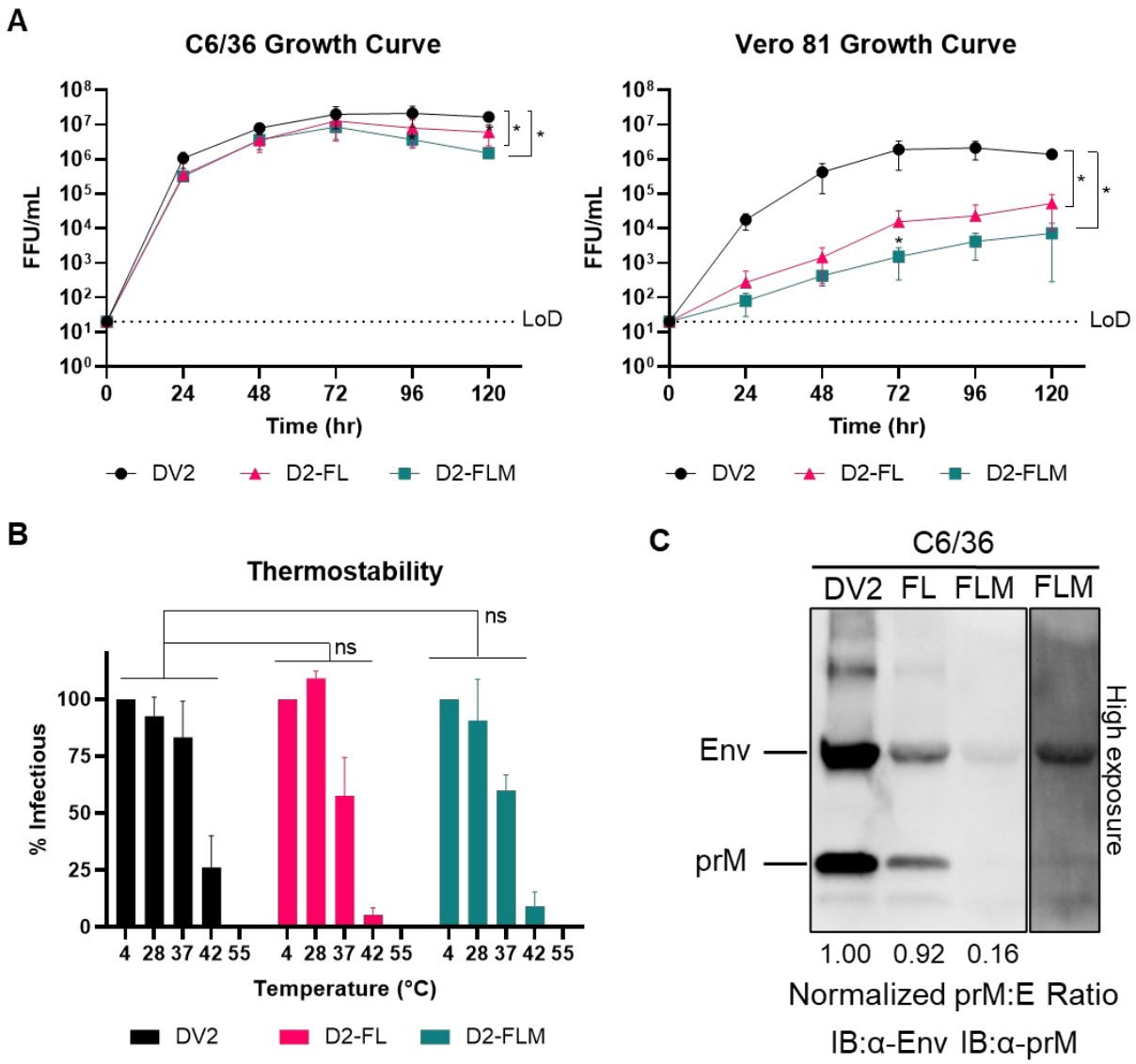

Figure 2: Biological and physical properties of mature DENV2 fusion loop mutants. A) Multistep growth curves (MOI = 0.05-0.1) of DV2-WT, D2-FL, and D2-FLM on C6/36 cells (left) or Vero 81 cells (right). B) Thermostability assay on DV2-WT, D2-FL, and D2-FLM. C) Western blot of virions, blotted against Envelope and prM proteins. The prM:E ratio was determined and normalized to the DV2-WT ratio. Averages of 3 biological replicates are shown. Two-way ANOVA was used for statistical comparison of growth curves and thermostability: ns = not significant; * < 0.05; ** < 0.005; *** < 0.0005.

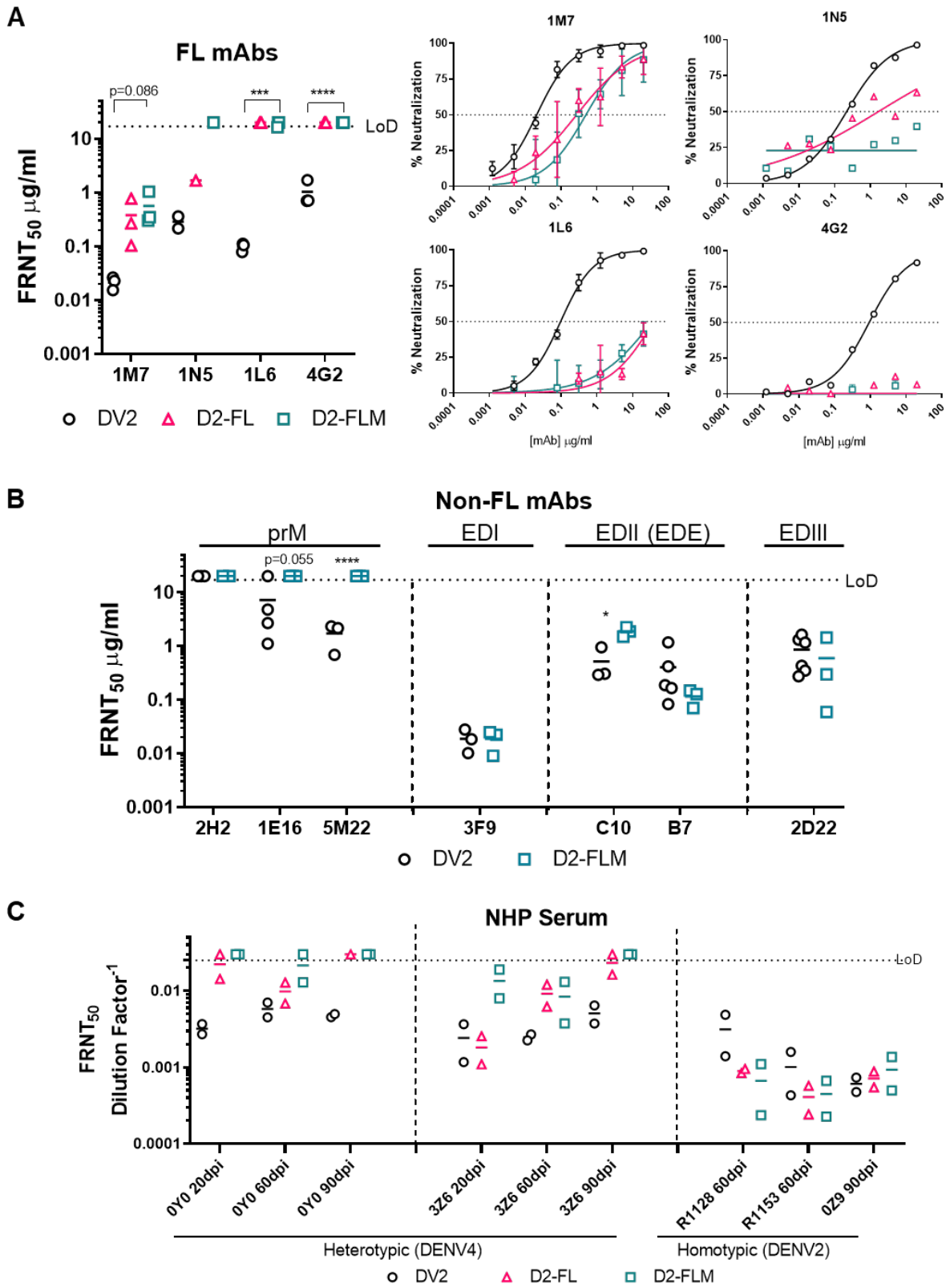
A
FL mAbs
p=0.086
***
****
LoD
FRNT50 µg/ml
1M7
1N5
1L6
4G2
DV2
D2-FL
D2-FLM
% Neutralization
[mAb] µg/ml
B
Non-FL mAbs
prM
EDI
EDII (EDE)
EDIII
p=0.055
****
*
2H2
1E16
5M22
3F9
C10
B7
2D22
C
NHP Serum
FRNT50 Dilution Factor-1
0Y0 20dpi
0Y0 60dpi
0Y0 90dpi
3Z6 20dpi
3Z6 60dpi
3Z6 90dpi
R1128 60dpi
R1153 60dpi
0Z9 90dpi
Heterotypic (DENV4)
Homotypic (DENV2)

363

364 **Figure 3**: Fusion loop mutant is insensitive to fusion loop mAbs, the major target for cross-
365 reactive Abs in NHPs. A) Left: $FRNT_{50}$ values for neutralization of DV2-WT, D2-FL, and
366 D2-FLM with mAbs against the FL (1M7, 1N5, 1L6, 4G2). All Abs were tested in at least
367 n=3 independent experiments, except 1N5 due to limited Ab. Right: Average
368 neutralization curves for neutralization of DV2-WT, D2-FL, and D2-FLM with mAbs
369 against the DENV2 fusion loop. B) $FRNT_{50}$ values for neutralization of DV2-WT and D2-
370 FLM with mAbs against DENV2 prM (2H2, 1E16, 5M22), EDI (3F9), EDE (C10, B7), and
371 EDIII (2D22). All Abs were tested in at least n=3 independent experiments. C)
372 Neutralization of DV2-WT, D2-FL, and D2-FLM with sera from NHPs infected with either
373 DENV4 or DENV2. $FRNT_{50}$s were compared using Student's t-test. Significant symbols
374 are as follows: *, $P < 0.05$; **, $P < 0.005$; ***, $P < 0.0005$; ****, $P < 0.00005$. The data are
375 graphed as means ± standard deviations.
376
377

Human #	Infected Serotype	**Collection Time**	**DV2**	**D2-FL**	**D2-FLM**
DS1500	DENV1	Convalescent serum	1 : 75	ND	1 : 53
DS2499			1 : 80	ND	1 : 52
DS1136	DENV3		1 : 133	ND	1 : 45
DS1160			1: 86	ND	1: 208
DS0275	DENV4		1: 94	ND	1 : 94
DS2239			1: 156	ND	1 : 42

NHP #	Infected Serotype	**Collection Time**	**DV2**	**D2-FL**	**D2-FLM**
R628	DENV4	30dpi	< 1:40	< 1:40	< 1:40
		60dpi	< 1:40	< 1:40	< 1:40
		90dpi	1 : 42*	< 1:40	< 1:40
R737		30dpi	< 1:40	< 1:40	< 1:40
		60dpi	< 1:40	< 1:40	< 1:40
		90dpi	< 1:40	< 1:40	< 1:40
R1132		30dpi	< 1:40	< 1:40	< 1:40
		60dpi	< 1:40	< 1:40	< 1:40
		90dpi	< 1:40	< 1:40	< 1:40
R1160		30dpi	1 : 58*	< 1:40	< 1:40
		60dpi	1 : 57*	1 : 50*	< 1:40
		90dpi	< 1:40	1 : 57*	1 : 91*

Table 1: Summary of $FRNT_{50}$s of human convalescent serum and NHP infection serum against DV2, D2-FL and D2-FLM.

381 **REFERENCES**

382 1. Bhatt, S. *et al.* The global distribution and burden of dengue. *Nature* **496**, (2013).
383 2. Brady, O. J. *et al.* Refining the Global Spatial Limits of Dengue Virus
384 Transmission by Evidence-Based Consensus. doi:10.1371/journal.pntd.0001760.
385 3. Ebi, K. L. & Nealon, J. Dengue in a changing climate. *Environ Res* **151**, 115–123
386 (2016).
387 4. Messina, J. P. *et al.* The current and future global distribution and population at
388 risk of dengue. *Nat Microbiol* doi:10.1038/s41564-019-0476-8.
389 5. Halstead, S. B. Pathogenesis of Dengue: Challenges to Molecular Biology.
390 *Science (1979)* **239**, 476–481 (1988).
391 6. Katzelnick, L. C. *et al.* Antibody-dependent enhancement of severe dengue
392 disease in humans. *Science (1979)* **358**, 929–932 (2017).
393 7. Rey, F. A., Stiasny, K., Vaney, M., Dellarole, M. & Heinz, F. X. The bright and the
394 dark side of human antibody responses to flaviviruses: lessons for vaccine
395 design. *EMBO Rep* **19**, 206–224 (2018).
396 8. Rabaa, M. A. *et al.* Genetic epidemiology of dengue viruses in phase III trials of
397 the CYD tetravalent dengue vaccine and implications for efficacy. *Elife* **6**, 1–22
398 (2017).
399 9. Raut, R. *et al.* Dengue type 1 viruses circulating in humans are highly infectious
400 and poorly neutralized by human antibodies. *Proc Natl Acad Sci U S A* **116**, 227–
401 232 (2019).
402 10. Lai, C. Y. *et al.* Analysis of Cross-Reactive Antibodies Recognizing the Fusion
403 Loop of Envelope Protein and Correlation with Neutralizing Antibody Titers in
404 Nicaraguan Dengue Cases. *PLoS Negl Trop Dis* **7**, 1–11 (2013).
405 11. Beltramello, M. *et al.* The human immune response to dengue virus is dominated
406 by highly cross-reactive antibodies endowed with neutralizing and enhancing
407 activity. *Cell Host Microbe* **8**, 271–283 (2010).
408 12. Costin, J. M. *et al.* Mechanistic Study of Broadly Neutralizing Human Monoclonal
409 Antibodies against Dengue Virus That Target the Fusion Loop. *J Virol* **87**, 52–66
410 (2013).
411 13. Wilder-Smith, A. *et al.* Personal View Deliberations of the Strategic Advisory
412 Group of Experts on Immunization on the use of CYD-TDV dengue vaccine The
413 Strategic Advisory Group of Experts (SAGE) on Immunization advises WHO on
414 global policies for vaccines. In. *Lancet Infect Dis* **19**, e31–e38 (2019).
415 14. Dengue vaccine: WHO position paper, September 2018 – Recommendations.
416 *Vaccine* **37**, 4848–4849 (2019).
417 15. Izmirly, A. M., Alturki, S. O., Alturki, S. O., Connors, J. & Haddad, E. K.
418 Challenges in Dengue Vaccines Development: Pre-existing Infections and Cross-
419 Reactivity. *Front Immunol* **11**, 1055 (2020).
420 16. Modis, Y., Ogata, S., Clements, D. & Harrison, S. C. Structure of the dengue virus
421 envelope protein after membrane fusion. *Nature* **427**, 313–319 (2004).
422 17. Klein, D. E., Choi, J. L. & Harrison, S. C. Structure of a Dengue Virus Envelope
423 Protein Late-Stage Fusion Intermediate. *J Virol* **87**, 2287–2293 (2013).

18. Smith, S. A. *et al.* The potent and broadly neutralizing human dengue virus-specific monoclonal antibody 1C19 reveals a unique cross-reactive epitope on the bc loop of domain II of the envelope protein. *mBio* **4**, (2013).
19. Rodenhuis-Zybert, I. A. *et al.* Immature Dengue Virus: A Veiled Pathogen? *PLoS Pathog* **6**, e1000718 (2010).
20. Tse, L. v. *et al.* Generation of Mature DENVs via Genetic Modification and Directed Evolution. *mBio* **13**, 1–18 (2022).
21. Smith, S. A. *et al.* Persistence of Circulating Memory B Cell Clones with Potential for Dengue Virus Disease Enhancement for Decades following Infection. *J Virol* **86**, 2665–2675 (2012).
22. Oliphant, T. *et al.* Antibody Recognition and Neutralization Determinants on Domains I and II of West Nile Virus Envelope Protein. *J Virol* **80**, 12149–12159 (2006).
23. Lai, C.-Y. *et al.* Antibodies to Envelope Glycoprotein of Dengue Virus during the Natural Course of Infection Are Predominantly Cross-Reactive and Recognize Epitopes Containing Highly Conserved Residues at the Fusion Loop of Domain II. *J Virol* **82**, 6631–6643 (2008).
24. Dejnirattisai, W. *et al.* Cross-Reacting Antibodies Enhance Dengue Virus Infection in Humans. *Science (1979)* **328**, 745–748 (2010).
25. Sharma, A. *et al.* The epitope arrangement on flavivirus particles contributes to Mab C10's extraordinary neutralization breadth across Zika and dengue viruses. *Cell* **184**, 6052-6066.e18 (2021).
26. Andrade, D. v. *et al.* Tracking the polyclonal neutralizing antibody response to a dengue virus serotype 1 type-specific epitope across two populations in Asia and the Americas. *Scientific Reports 2019 9:1* **9**, 1–12 (2019).
27. Young, E. *et al.* Identification of Dengue Virus Serotype 3 Specific Antigenic Sites Targeted by Neutralizing Human Antibodies. (2020) doi:10.1016/j.chom.2020.04.007.
28. Gallichotte, E. N. *et al.* A new quaternary structure epitope on dengue virus serotype 2 is the target of durable type-specific neutralizing antibodies. *mBio* **6**, (2015).
29. Barba-Spaeth, G. *et al.* Structural basis of potent Zika–dengue virus antibody cross-neutralization. *Nature 2016 536:7614* **536**, 48–53 (2016).
30. Dejnirattisai, W. *et al.* A new class of highly potent, broadly neutralizing antibodies isolated from viremic patients infected with dengue virus. *Nature Immunology 2014 16:2* **16**, 170–177 (2014).
31. Kotaki, T. *et al.* An affinity-matured human monoclonal antibody targeting fusion loop epitope of dengue virus with in vivo therapeutic potency. *Sci Rep* **11**, 1–14 (2021).
32. de Alwis, R. *et al.* Dengue Viruses Are Enhanced by Distinct Populations of Serotype Cross-Reactive Antibodies in Human Immune Sera. *PLoS Pathog* **10**, e1004386 (2014).
33. Rouvinski, A. *et al.* Covalently linked dengue virus envelope glycoprotein dimers reduce exposure of the immunodominant fusion loop epitope. *Nat Commun* **8**, (2017).

469 34. Rockstroh, A. *et al.* Recombinant Envelope-Proteins with Mutations in the
470 Conserved Fusion Loop Allow Specific Serological Diagnosis of Dengue-
471 Infections. *PLoS Negl Trop Dis* **9**, 1–12 (2015).
472 35. Slon-Campos, J. L. *et al.* A protective Zika virus E-dimer-based subunit vaccine
473 engineered to abrogate antibody-dependent enhancement of dengue infection.
474 *Nature Immunology 2019 20:10* **20**, 1291–1298 (2019).
475 36. Metz, S. W. *et al.* In Vitro Assembly and Stabilization of Dengue and Zika Virus
476 Envelope Protein Homo-Dimers. *Scientific Reports 2017 7:1* **7**, 1–8 (2017).
477 37. Kudlacek, S. T. *et al.* Designed, highly expressing, thermostable dengue virus 2
478 envelope protein dimers elicit quaternary epitope antibodies. *Sci Adv* **7**, (2021).
479 38. Zhang, S. *et al.* A mutation in the envelope protein fusion loop attenuates mouse
480 neuroinvasiveness of the NY99 strain of West Nile virus. *Virology* **353**, 35–40
481 (2006).
482 39. Tian, Y., Grifoni, A., Sette, A. & Weiskopf, D. Human T Cell Response to Dengue
483 Virus Infection. *Front Immunol* **10**, 2125 (2019).
484 40. Ngono, A. E. & Shresta, S. Cross-reactive T Cell immunity to dengue and zika
485 viruses: New insights into vaccine development. *Front Immunol* **10**, 1316 (2019).
486 41. Waickman, A. T. *et al.* Dissecting the heterogeneity of DENV vaccine-elicited
487 cellular immunity using single-cell RNA sequencing and metabolic profiling.
488 *Nature Communications 2019 10:1* **10**, 1–16 (2019).
489 42. Gallichotte, E. N. *et al.* Genetic Variation between Dengue Virus Type 4 Strains
490 Impacts Human Antibody Binding and Neutralization. *CellReports* **25**, 1214–1224
491 (2018).
492 43. Halstead, S. B. & Marchette, N. J. BIOLOGIC PROPERTIES OF DENGUE
493 VIRUSES FOLLOWING SERIAL PASSAGE IN PRIMARY DOG KIDNEY CELLS:
494 STUDIES AT THE UNIVERSITY OF HAWAII. *Am J Trop Med Hyg* **69**, 5–11
495 (2003).
496 44. Juraska, M. *et al.* Viral genetic diversity and protective efficacy of a tetravalent
497 dengue vaccine in two phase 3 trials. *Proc Natl Acad Sci U S A* **115**, E8378–
498 E8387 (2018).
499 45. Messer, W. B. *et al.* Development and characterization of a reverse genetic
500 system for studying dengue virus serotype 3 strain variation and neutralization.
501 *PLoS Negl Trop Dis* **6**, (2012).
502 46. Tse, L. V. *et al.* Structure-guided evolution of antigenically distinct adeno-
503 associated virus variants for immune evasion. *Proc Natl Acad Sci U S A* **114**,
504 E4812–E4821 (2017).
505